Diffuse Optical Tomography based on Simplified Spherical Harmonics Approximation

Michael Chu[1] and Hamid Dehghani[2]
[1] *School of Physics, University of Exeter, United Kingdom*
[2] *School of Computer Science, University of Birmingham, United Kingdom*
h.dehghani@cs.bham.ac.uk

Abstract: The use of higher order approximations to the Radiative transport equation, through simplified spherical harmonics expansion (SP_N) in optical tomography are presented. At higher orders, the image reconstruction becomes highly under-determined due to the large increase in the number of unknowns which cannot be adequately recovered. However, reconstruction of diffuse parameters, namely optical absorption and reduced scatter have shown to be more accurate where only the sensitivity matrix used in the inverse problem is based on SP_N method and image reconstruction is limited to these two diffuse parameters.

OCIS codes: (100.3190) Inverse problems; (170.3660) Light propagation in tissues;

1. Introduction

The use of biological markers for function specific optical imaging has led to the development of novel imaging systems and algorithms that aim to recover images of function specific activity within small animals using, for example, fluorescence [1] or bioluminescence markers [2, 3]. Most NIR imaging systems rely on the use of a model based image reconstruction algorithm in which the light distribution within the imaging domain is approximated to provide a match to measured boundary data. The most commonly applied model for the estimation of NIR light propagation in tissue is achieved through the Diffusion Approximation (DA) to the Radiative Transport Equation (RTE) through its robustness in implementation and computational speed and flexibility. To accurately model NIR light propagation in small geometries, or models with high absorption (such as for bioluminescence imaging), higher ordered forward models are needed whereby the problem is no longer limited by the 'diffuse' approximation. The application of Simplified Spherical Harmonics (SP_N) approximation to the RTE has been previously applied and studied [4, 5] and have been demonstrated to give accurate solutions for small geometries and in cases where the source/detector separation is small.

The vast majority of existing model based reconstruction algorithms make use of the DA [6, 7]. The image reconstructions therefore aim to form images of the absorption coefficient, μ_a and the diffusion coefficient $\kappa = 1/3(\mu_a+\mu_s')$ where $\mu_s'=(1-g)\mu_s$ and μ_s and g are the scattering coefficient and anisotropic factor respectively. There are been limited work on the feasibility of using higher order SP_N methods in image reconstruction, whereby the number of unknowns increase for each increased order of the approximation. In this study, SP_N based models are used to present a framework for image reconstruction in NIR imaging, whereby the parameters to be reconstructed are limited to absorption and reduced scattering coefficient.

2. Methods and Results

SP_N based image reconstruction algorithms have been developed for N=1, 3, 5 and 7 using the modified Tikhonov minimization method. If we assume that the composite moments of fluence are measureable, the SP_N approximation introduces the possibility of reconstructing a wider range of optical parameters, Table 1. Test boundary data was generated using a 2D circular geometry of radius 43 mm, with μ_a = 0.01 mm^{-1}, μ_s = 10 mm^{-1}, and g = 0.9. A highly absorbing anomaly, with μ_a = 0.02 mm^{-1} and a highly scattering anomaly with μ_s = 20 mm^{-1}, were inserted, Figure 1. Each of the SP_N reconstruction algorithms (for N = 1, 3, 5 and 7) is capable of reconstructing different optical properties, depending on the order N. In order to test the capability of each of the SP_N models, the optical properties listed in Table 1 were reconstructed, and from these, values of μ_a and μ_s were extracted [5]. For the inverse model, the same mesh as the forward model was used without added noise to ensure that any errors in the reconstructed optical maps were *only* due to the complexity of the higher ordered approximations.

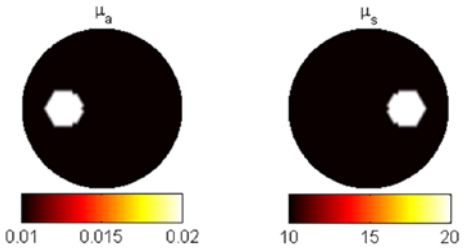

Figure 1. FEM target model

Figure 2(a) shows the reconstructed images generated using an SP_1 based reconstruction algorithm and SP_1 forward data. The location of the two anomalies has been accurately reconstructed. The background optical

properties have been accurately recovered although the values of the two anomalies have been over-estimated. The reconstructed image shows a maximum absorption coefficient of 0.0249 mm^{-1} and a maximum scattering coefficient of 23.9 mm^{-1}. The SP_1 reconstruction required 32 iterations at 3.1 second per iteration to recover the two relevant unknowns.

Table 1. Reconstructed values of SP_N algorithms where the diffusion terms $\kappa_n=1/(A\mu_{an})$ and A is a constant.

Reconstruction model	Forward data used	Unknown parameters
SP_1	SP_1	κ_1, μ_a
SP_3	SP_3	κ_1, κ_3, μ_{a1}, μ_{a2}
SP_5	SP_5	κ_1, κ_3, κ_5, μ_{a1}, μ_{a2}, μ_{a4}
SP_7	SP_7	κ_1, κ_3, κ_5, κ_7,μ_{a1}, μ_{a2}, μ_{a4}, μ_{a6}

The SP_3 reconstruction (using SP_3 data) Figure 2(b) has also accurately recovered the location and shape of the two anomalies. The recovered absorption and scattering coefficients have underestimated the target values, returning 0.0189mm^{-1} and 17.3mm^{-1} respectively. Unlike the SP_1 image, the SP_3 reconstruction shows signs of cross talk between the absorption and scattering images. The SP_3 reconstruction required 13 iterations at 7.3 second per iteration to recover the four relevant unknowns.

Reconstruction using the SP_5 model (using SP_5 data) is shown in Figure 2(c). In this case, the optical properties have again been overestimated with a maximum absorption coefficient of 0.0224mm^{-1} and a maximum scattering coefficient of 21.4mm^{-1}. The cross talk between the absorption and scattering images is still present. The SP_5 reconstruction required 34 iterations at 54 second per iteration to recover the six relevant unknowns.

The optical maps generated by the SP_7 model (using SP_7 data), Figure 2(d) contains artifact throughout the domain. The location of the highly absorbing target has been recovered with poor size and contrast accuracy. The reconstruction failed to recover the highly scattering target. It is likely that the failure of the SP_7 reconstruction is due to the highly under-determined nature of the problem. The SP_7 model requires 8 unique variables to be calculated at each node, i.e. 14280 unknowns, based on just 1920 boundary measurements. The SP_7 reconstruction required 20 iterations at 52 second per iteration to recover the eight relevant unknowns.

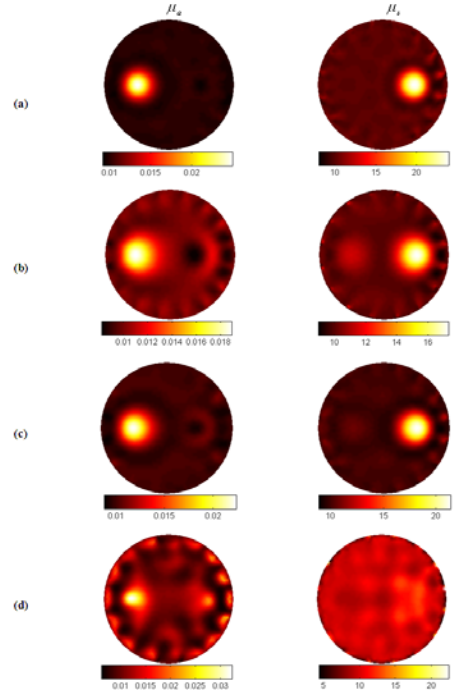

Figure 2: Reconstructed optical maps using a) SP_1, b) SP_3, c) SP_5, d) SP_7 based reconstruction algorithms

The SP_N approximations are based on composite moments of fluence with the total flux calculated from weighted sum of these components [5]. The SP_N reconstruction algorithms used above were therefore based on various moments of the phase and amplitude boundary data which attempted to recover all moments of absorption and scattering coefficients. In practice, however, there are no experimental methods to easily measure the angular components of amplitude and phase and so image reconstructions must be based on total values of fluence. A new reconstruction algorithm was therefore developed that used the SP_N model but only required measurements of phase and amplitude as available from the total fluence and not composite moments. The new reconstruction algorithm uses the SP_5 forward model to calculate the composite moments of fluence. The Jacobian is then constructed where log of amplitude and absolute phase are extracted from the calculated total fluence from the SP_N model. By eliminating the composite moments of fluence, however, it is only possible to reconstruct for μ_a. and μ_s (assuming g = 0.9). This new reconstruction algorithm is tested using SP_5 forward data and the resulting optical map is shown in Figure 3(a). The reconstruction has performed well, recovering the optical parameters within 10% of the target

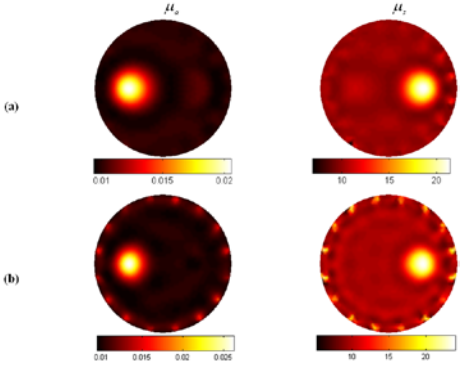

Figure 3: Diffusion based images from SP_5 data using (a) SP_5 based Jacobian and (b) SP_1 based Jacobian.

values. For comparison, the same forward data is also used to reconstruct optical parameters using the DA based algorithm, Figure 3(b). In this case, the target values have been over-estimated and boundary artifact has been introduced, indicating the maximum errors seen from high order model mismatch, is as expected near the source / detector positions, which lead to image inaccuracy and artifacts.

3. Discussions and conclusions

Reconstruction algorithms based on the SP_N approximation have been developed and tested. For image reconstruction, the same FEM model as for the forward data was used and no noise was added. It is shown, Figure 2(a)-(c), that for N=1, 3 and 5 the reconstructions performed well, with the reconstructed values being within 24% of expected values with the worse results being obtained from SP_1 and absorption coefficient. This accuracy could be further improved by the optimization of the regularization parameter and stopping criteria. The N=7 model, however, failed to accurately recover the target values, Figure 2(d). The absorption coefficient, although located, is extremely over estimated, with some cross-talk from the scattering value. The reconstructed scatter image contains high valued artifacts and can be considered inaccurate. By limiting the presented results to these larger domains, it is also worth noting that the majority of image artifacts are seen at the boundary, near the source locations, where SP_1 solution is known to be less accurate. It is therefore expected that the errors seen due to the lack of higher order approximations to be substantially more significant in small geometry imaging experiments. The poor performance of the SP_7 model was most likely due to the under-determined nature of the problem. As stated earlier, the SP_7 model contains 8 unique unknown variables which need to be calculated at each spatial location (FEM node), i.e. 14280 unknowns, based on just 1920 boundary measurements (240 log amplitude and 240 Phase, based on 16 co-located source and detectors and 4 composite moments of fluence).

The SP_N equations are based on composite moments of fluence [5]. In reality, however, experimental systems can only measure the total fluence at the boundary of the domain and so the full SP_N reconstruction algorithms are of limited use in image reconstruction where all composite moments are needed. An alternative method has been proposed in which the forward models are based on absolute fluence but the Jacobian matrix was calculated using the SP_5 model to allow the calculation of absorption (μ_a) and scattering (μ_s) coefficient only. The diffusion parameter based images reconstructed from simulated SP_5 data whereby the Jacobian is based on either SP_1 or SP_5, Figure 3, indicate that although both models can be used, the higher order model is more accurate both in terms of quantitative and qualitative analysis. The target values of the test problem calculated using SP_5 are recovered with more accuracy as compared to the SP_1 based model with much less artifact. Additionally, eliminating the use of complex moments also results in decreased computation time and memory requirements.

The results presented in this work indicate that for image reconstruction whereby the DA is less valid, in for example, small animal imaging and / or where the absorption coefficient is more dominant, the higher order models based on simplified spherical harmonics can be used to generate the sensitivity matrix for diffusion based image reconstruction, without the additional computation complexity in terms of the number of unknown parameters. The incorporation of these more accurate models can however allow for a better accuracy in terms of light propagation models.

4. Acknowledgements

This work has been sponsored by EPSRC UK.

5. References

1. Davis, S.C., et al., *Magnetic resonance-coupled fluorescence tomography scanner for molecular imaging of tissue.* Rev Sci Instrum, 2008. 79(6): p. 064302.
2. Kuo, C., et al., *Three-dimensional reconstruction of in vivo bioluminescent sources based on multispectral imaging.* JBO, 2007. 12: p. 24007.
3. Dehghani, H., S.C. Davis, and B.W. Pogue, *Spectrally resolved bioluminescence tomography using the reciprocity approach.* Med Phys, 2008. 35(11): p. 4863-71.
4. Klose, A.D. and E.W. Larsen, *Light transport in biological tissue based on the simplified spherical harmonics equations.* Journal of Computational Physics, 2006. 220(1): p. 441-470.
5. Chu, M., et al., *Light transport in biological tissue using three-dimensional frequency-domain simplified spherical harmonics equations.* phys med biol, 2009. 54(8): p. 2493-509.
6. Arridge, S.R., *Optical tomography in medical imaging.* Inverse Problems, 1999. 15(2): p. R41-R93.
7. Dehghani, H., et al., *Near Infrared Optical Tomography using NIRFAST: Algorithms for Numerical Model and Image Reconstruction Algorithms.* Communications in Numerical Methods in Engineering, 2008.